JEM

Journal of Electron Microscopy **60(Supplement 1)**: S269–S278 (2011)
doi: 10.1093/jmicro/dfr027

60th Anniversary Issue: Physical

Picoscale science and nanoscale engineering by electron microscopy

Zhong Lin Wang*

School of Materials Science and Engineering, Georgia Institute of Technology, Atlanta, GA 30332-0245, USA
*To whom correspondence should be addressed. E-mail: zhong.wang@mse.gatech.edu

Abstract A future scanning/transmission electron microscope is proposed to be a comprehensive machine that is capable of providing picoseconds time-resolved information at sub-nanometer scale and even at picometer scale, spatial resolution. At the same time, physical and chemical properties can be measured *in situ* from a region as small as a few nanometers by introducing local electric, mechanical, thermal, magnetic and/or optical stimulations/excitations under vacuum or even in a quasi-ambient environment. It is anticipated that nanoscopy and picoscopy will be key tools for studying picoscale science and developing nanoscale technology related to materials science, biology, physics and chemistry.

Keywords *In situ* electron microscopy, nanoscopy, picoscopy

Received 6 January 2011, accepted 25 March 2011

Introduction

The discovery and development of X-ray-based technology is one of the most important inventions in human history, which has a tremendous impact on numerous fields such as material science, physics, biology and medicine. In parallel to X-ray diffraction and imaging, electron beam based science and technology is being developed as the most powerful tool for exploring picometer and picosecond scale phenomena. The traditional electron microscopy is being replaced by nanoscopy and even picoscopy to reflect the resolution provided by electron beam technologies. The future developments of electron microscopy are likely to be in the directions of super high image and probe resolution, picosecond time-resolved phenomena, *in situ* nanoscale physical property measurements and environmental stimulated chemical and surface processes.

The impact of electron microscopy has largely been expanded especially since the kick off of the nanotechnology initiatives in 2000. By combining the powerful imaging and diffraction techniques with the *in situ* measurements, electron microscopy has played a key role in nanomechanics, nanoelectronics and nanomaterials. By introducing the environmental transmission electron microscopy (TEM), it is feasible to directly real-time image the chemical processes occurring at sample surfaces under realistic practical environment under which the samples will be used in practical applications. The objective of this paper is to give a summary of the techniques being developed relevant to TEM in presenting its possible prospects of studying picoscale science and nanoscale engineering.

Picometer imaging, diffraction and spectroscopy

The original idea of developing electron microscopy in 1928 was to directly image an object in order to provide a resolution better than that of optical microscopy. Direct imaging of dislocations in thin metal foils in the 1950–1960s provided direct evidence about the mechanisms proposed for creeping and fatigue in metals [1]. The development of high-resolution lattice imaging in 1960–1980s with an

image resolution of ~0.2 nm has been a key tool in studying the structure of modern materials [2–4]. At the same time, the corresponding development of analytical tools, such as energy-dispersive X-ray spectroscopy (EDS) [5] and electron energy-loss spectroscopy (EELS) [6], provides powerful analytical tools for revealing the chemical and electronic structures of materials.

The image resolution in a transmission electron microscope (TEM) was limited by the presence of spherical aberration, but this barrier has been broken with the development of the C_s-corrected TEM, with the possibility of providing an image resolution below 0.1 nm [7, 8]. The feasibility of achieving picometer resolution makes it possible to directly image light elements in inorganic materials [9, 10], polarization in ferroelectric thin films [11], structures of nanoparticles [12] and surface single-atom imaging [13].

A high-resolution TEM image is formed by the coherently scattered electron beams, is largely dominated by phase contrast and is less sensitive to the atomic number. With the increase in the aperture size for acquiring high-resolution information, the contribution made by phonon-scattered electrons in the TEM image becomes very significant and unavoidable [14–18], but the image formed by phonon-scattered or thermal diffuse scattered electrons is not included in the simulation of traditional multislice theory [19], resulting in a large difference in image contract between the experimentally received images and the simulated ones. In such a case, new theories including phonon-scattered electrons in the image simulation are required for quantitative structure analysis [15, 20–22]. But such commercial software is still unavailable.

The well-established theories for electron diffraction and imaging are the Bloch wave theory and multislice theory. With the improvement in precision and resolution of information provided by today's microscopy, it is mandatory to explore new theoretical approaches for image simulations by including inelastic scattering [23–25]. Although an energy filter can be applied in data acquisition to filter away the contribution made by plasmon and single-electron excitations, phonon-scattered electrons are still present in images and diffraction patterns except in off-axis holograms [26, 27]. The inclusion of a Debye–Waller factor in the scattering factor takes care of only the absorption effect to the elastic wave and does not include the contribution made by the phonon-scattered electrons to the image!

The development of scanning transmission electron microscopy (STEM) starting from the 1970s has been a major thrust for exploring new imaging tools [28, 29]. In complementary to the powerful bright-field imaging in TEM, the dark-field imaging in STEM has made it unique in a number of important applications, such as chemical imaging, single-atom imaging and structure at grain boundaries [30, 31], by taking the advantage provided by the fine probe of <0.2 nm. The high-angle annular dark-field (HAADF) STEM imaging takes the advantages of the high-angle scattered electrons as a result of highly localized phonon scattering process for forming the image [32], so that the image contrast is directly related to the projected atomic number in the atom column [33].

The HAADF STEM imaging takes the advantages offered by the phonon-scattered electrons so that it carries the characteristics of partial coherent imaging. This is the case for a perfect crystal structure. For the case of grain boundary where nonperiodic or 'disorder' structure is present, diffuse scattering at a high angle can be generated by local structural distortion or strain [34], which is the Huang scattering. Therefore, the local image contrast may be slightly different from the expected result and may not be directly related to the projected atomic number as simple as it appears especially with the presence of a strong diffraction effect. One has to be cautious in image interpretation. In general, although the image interpretation for HAADF STEM is relatively straightforward, image simulation including a dynamic effect is needed in some cases for quantitative structure analysis.

In parallel to super-high-resolution imaging, spectroscopy with an energy resolution of a few meV is being developed, which will be powerful enough to resolve phonon spectra, to fully investigate the solid-state structure in a capacity comparable to synchrotron radiation. The high-energy resolution is achieved by using an energy filter while preserving the intensity of the incident electron beam.

Picosecond imaging, diffraction and spectroscopy

The traditional electron microscopy relies on a 'static' image so that the information provided is a time-averaged structure of a dynamic configuration within a few ms at the most. It is generally believed that 'one picture is equivalent to thousands of words', and by the same token, 'one movie is equivalent to thousands pictures'. Developing time-resolved microscopy is equivalent to revealing a physical process by a video at a time resolution of picoseconds. By using pulse laser-excited electron emission process at a tip, the duration and interval between electrons 'packet' can be precisely controlled by the laser pulses [35, 36].

A revolutionary development by Prof A. Zewail's group is the four-dimensional electron microscopy by imaging in space and time. The main idea is to split a femtosecond laser beam into two: one is directed to the electron gun for generating the incident electron packet, which serves as a 'shutter' for capturing the dynamic process; the other beam, with a controlled delay in time, is directed to excite the sample [1]. By controlling the delay time Δt between the excitation of the event in the specimen and the exposure of the sample to the electron packet/pulse for imaging, an instantaneous structure of the sample at Δt is captured. Structural dynamics of ZnO nanowire arrays were obtained from the diffraction frames at different delay times after the optical excitation [37]. The nanowires grow along the *c*-axis with a uniform geometry. The corresponding electron diffraction was taken at a specific time after the laser excitation. The intensity decrease and the vertical spot movement for each Bragg spot were evident in the diffraction. All of the diffraction spots move downward at early times and recover the original positions at longer times. Typical behavior is shown for the (006) Bragg spot: whereas the intensity and vertical width are very similar in behavior and nearly recover (Fig. 1a) in only 200 ps, the rise in expansion along the *c*-axis is delayed by ~15 ps and decays on a much longer time scale, reaching completion in about 1 ns. The fluence dependence of the expansion, intensity and width indicates the role of the (electron–hole) carriers. The maximum *c*-axis expansion is plotted as a function of fluence (Fig. 1b). The energy of the exciting photon is less than half of the energy gap of ZnO (3.37 eV). Thus, the carriers are generated in the ZnO nanowires by energetically allowed three-photon excitation and/or by enhanced two-photon absorption. A single-photon absorption can excite phonons in the lattice. The transient status of structural changes has been captured [38]. The four-dimensional electron microscopy will be a major direction in electron microscopy science and

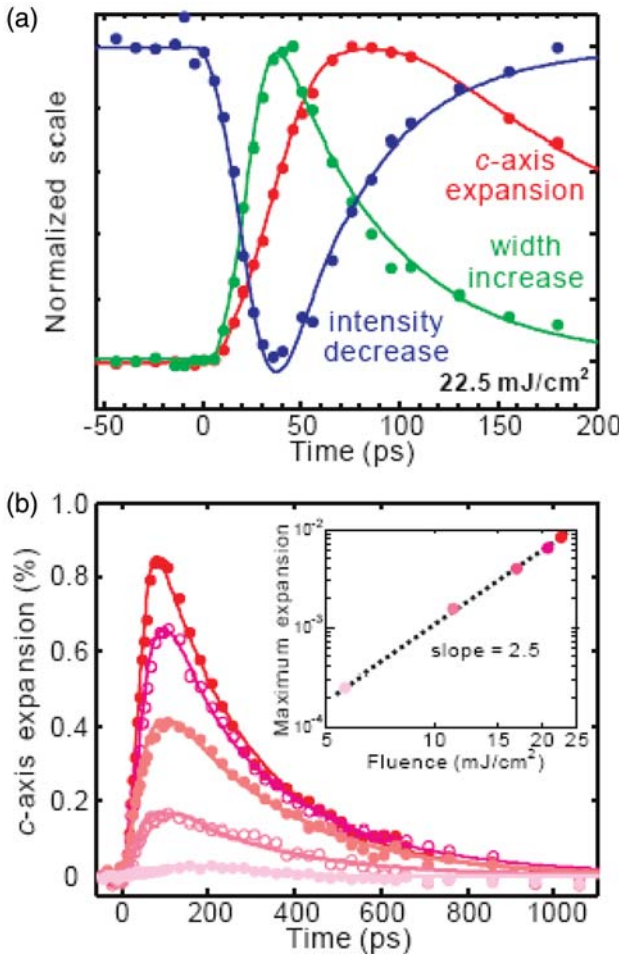

Fig. 1. Structural dynamics revealed by time-resolved electron microscopy. Changes of the *c*-axis expansion, diffraction intensity and vertical width of the (006) Bragg spot of ZnO nanowire arrays with time after being excited by a laser beam (with energy smaller than the bandgap of ZnO) at $t = 0$. (a) The intensity decrease (blue dots) and width increase (green dots) behave similarly and precede the buildup of structural expansion (red dots). In ~200 ps the former two diffraction features almost recover the original values, whereas the decay of expansion appears on a longer time (ns) scale. (b) A significantly larger *c*-axis expansion was obtained at higher excitation fluences. The fitted slope in the log–log plot (inset) indicates that the maximum expansion is proportional to the fluence to the power of 2.5. All solid lines are fits to the data [37].

it will impact the fundamentals in physics, chemistry and biology.

Nanoscale *in situ* measurements

Seeing is believing! *In situ* TEM is a direct approach for simultaneously revealing the structure and the corresponding physical/chemical process as it is occurring. The traditional *in situ* TEM is about a temperature driven structural changing process, such as phase transformation, crystal growth, mass diffusion [39] and surface reaction [40]. *In situ* TEM has largely been expanded to the area of physical

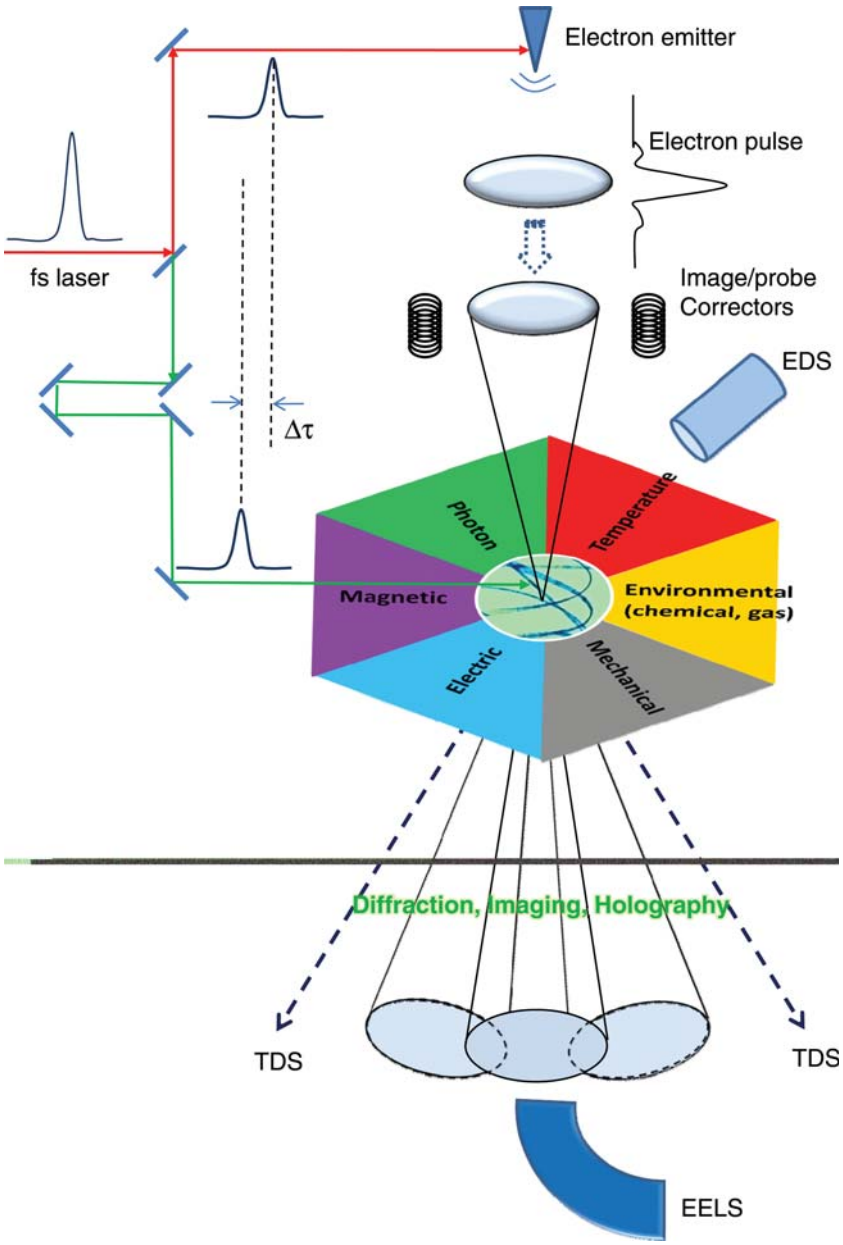

Fig. 2. Schematic diagram showing a 'dream' TEM/STEM for the future. The electron source is a picosecond time-resolved beam that can reveal dynamic processes at ~ps time resolution, which is excited and controlled by a femtosecond laser beam. The microscope is equipped with C_s and C_c correctors for generating 'aberration-free' electron imaging and fine probe at picometer-scale. The microscope is equipped with an energy filter that is capable of providing a high brightness electron beam with an energy resolution of a few meV for a high-resolution EELS study. Furthermore, a set of comprehensive specimen holders are available for studying the electrical, mechanical, magnetic, temperature and even phonon excited physical processes in the sample. An environmental specimen chamber is possible for studying chemical and surface processes at ambient conditions under which the sample will be used in practice. Furthermore, structural information is revealed by quantitative electron imaging, diffraction and holography. Chemical and electronic structure information is provided by energy-dispersive X-ray spectroscopy (EDS) and high-resolution electron energy-loss spectroscopy (EELS).

property measurement following the first demonstration of mechanical property measurement of a single-carbon nanotube in 1999 [41, 42]. TEM is now a comprehensive machine for nanoscale measurements with the possibility of introducing mechanical, electrical, magnetic, photonic and/or thermal stimulations (Fig. 2). In conjunction with the atomic-resolution imaging capability, *in situ* TEM is a powerful tool for studying and understanding the physical and chemical properties of a solid material at a high spatial resolution. Recently, *in situ* TEM is becoming an active field of research that is directly related to materials science, nanomechanics and nanoelectronics [43].

The core to the *in situ* TEM measurements is to build a sample holder through which a controlled force or field can be applied to a local region [44]. Various sample holders are being developed for various measurements. The key challenge is to quantify the applied force or field so that the measured physical properties can be understood quantitatively.

Mechanical properties

The elastic modulus of a carbon nanotube was first measured using a sample holder through which an external voltage was applied between a free-standing nanotube and a counter electrode. The force acting on the nanotube is directly proportional to the applied voltage. If we adjust the frequency of the applied voltage so that it matches the resonance frequency of the nanotube, then the nanotube would resonantly vibrate as judged from its projected image under the electron beam (Fig. 3). The elastic modulus of the nanotube is thus received from the observed resonance frequency. This first demonstration of field-induced resonance allows a direct application of TEM in nanomechanics [45], and it opens the field of *in situ* measurements in TEM.

Nanoindentation to measure the hardness of a thin film while the creation and movement of dislocations being observed simultaneously has also been illustrated [46–49]. *In situ* TEM has been applied to study the deformation mechanism of nanocrystalline metallic thin films [50, 51] and is an exciting approach toward nanomechanics.

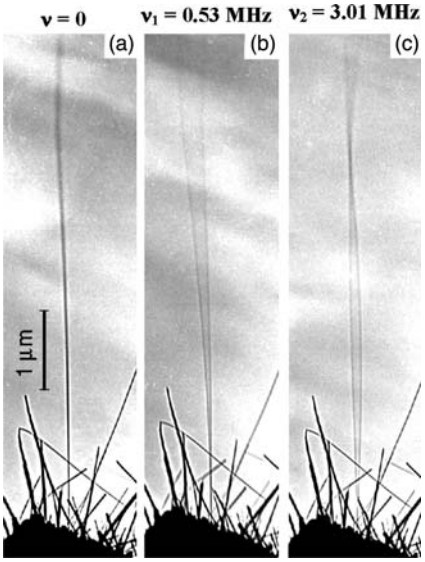

Fig. 3. Measuring the bending modulus of a carbon nanotube by an electric field-induced mechanical resonance phenomenon. (a) A nanotube at stationary; (b, c) the nanotube is at the first and second harmonic resonance as stimulated by an externally applied electric field at specific frequencies. This study stimulated the development of nanomeasurement techniques in TEM (from [41]).

Plastic deformation is an important mechanical property of engineering materials. The deformation behavior of a single-crystalline nanowire, for example, was investigated by *in situ* TEM. Due to the complex geometry of the scattered nanowires on a TEM grid and the curl broken supporting thin film on the grid, many nanowires can be bent or stretched as the supporting films are being stretched, using which the plastic deformation behavior of a nanowire is studied. As for SiC nanowires, an unusually large-strain plasticity of ceramic SiC nanowires at temperatures close to room temperature was directly observed [52]. The continuous plasticity of the SiC nanowires is accompanied by a process of increased dislocation density at an early stage, followed by an obvious lattice distortion, and finally reaches an entire structure amorphization at the most strained region of the NW. Super high plastic deformation was also observed for Si nanowires [53] and SiO_2 nanowires [54].

Electric transport properties

Measuring electric transport properties of a nanotube/nanowire is important for understanding its electrical characteristics. It is usually done using the two-point or four-point contact methods, in

which the contacting electrodes are fabricated using lithography, and the nanotube is laid down in between the electrodes. *In situ* property measurement gives the opportunity to directly correlate the observed electric property with the structure of the nanotube. The measurement was first done using a modified specimen holder, in which a carbon nanotube is in contact with a soft metal, such as a tiny mercury droplet (Fig. 4) [42, 55], so that a voltage can be applied. More significantly, all powerful functions of TEM including the atomic scale high-resolution imaging and spatially resolved chemical composition analysis using EDS and EELS could be particularly conducted on the strained region being tested or positions at which the electrons are being transported.

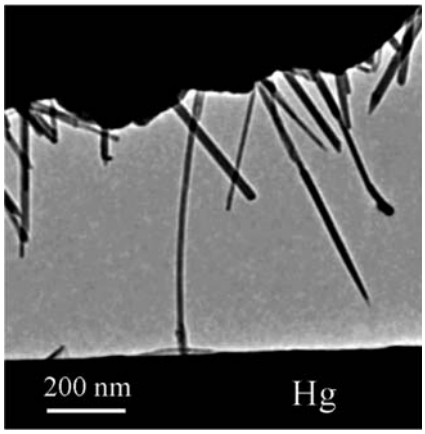

Fig. 4. *In situ* observation of electric transport through a single-carbon nanotube (from [42]).

Chemical processes and environmental properties

Environmental electron microscopy is experiencing a rapid development in recent years because there is a strong interest to directly study the sample at conditions under which it will be used in a practical surface or in catalytic processes. Instead of deriving the surface information under vacuum condition, it is vitally important to understand the realistic surface processes in a liquid or a gas environment [56–59]. Such studies are important for directly visualizing the growth process of a carbon nanotube, nanoparticle or nanowire in a gas or a liquid environment [60–62], providing an in-depth understanding about the surface physical and chemistry processes. Environmental microscopy will be an important direction of electron microscopy.

Direct observation of the location, state and function of a promoter in heterogeneous catalysis is critical in understanding the surface processes in catalysis. Figure 5 shows the high-resolution TEM image Cu nanocrystals supported on a ZnO substrate at a pressure of 1.5 and 5.0 mbar in a composed gas environment and at $T = 220°C$ [57]. The

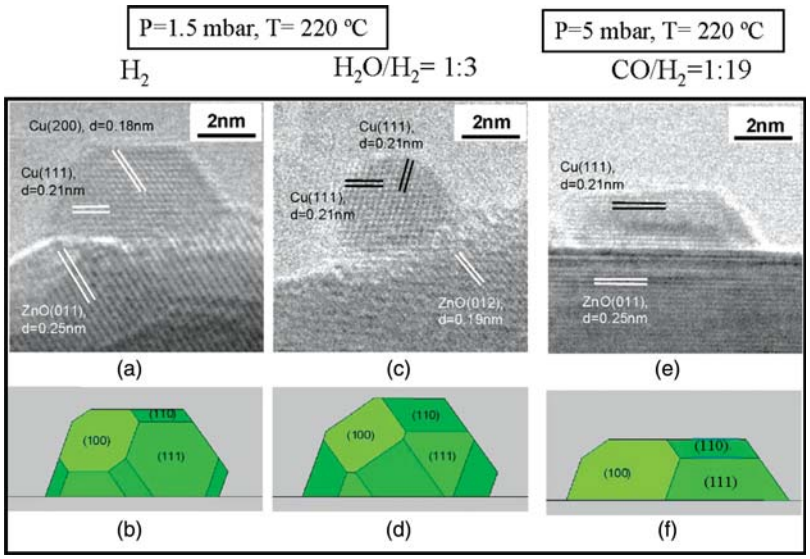

Fig. 5. *In situ* TEM images (a, c and e) of a Cu/ZnO catalyst in various gas environments together with the corresponding Wulff constructions of the Cu nanocrystals (b, d and f). (a) The image was recorded at a pressure of 1.5 mbar of H_2 at 220°C. The electron beam is parallel to the [011] zone-axis of copper. (c) Obtained in a gas mixture of H_2 and H_2O, H_2: H_2O = 3:1 at a total pressure of 1.5 mbar at 220°C. (e) Obtained in a gas mixture of H_2 (95%) and CO (5%) at a total pressure of 5 mbar at 220°C (from [57]).

particle shapes can be identified through the lattice images observed directly. For face-centered cubic (fcc) structured metals, the surfaces of the particles can be described by the Wulff construction with the inclusion of {111}, {100} and {110} types facets. The proportions of the {100} and {110} are significant at 1.5 mbar pressure, while these faces are greatly reduced after the pressure increases to 5 mbar. The change in the crystal facets surrounding the particles significantly affects their catalytic behavior.

Electro-mechanical coupled properties

A TEM equipped with a piezo-driven stage allows manipulating the specimen at a nanometer scale. Conductive electrodes can be embedded in the piezo-driven TEM holder so that a mechanical straining can be applied while the electrical transport properties are being measured. The first beautiful demonstration of coupling mechanical straining with electrical transport measurement was done for a Au contact, by revealing the quantum transport along the atom chains as the chain width decreases column by column [63, 64]. One-dimensional nanomaterials are the ideal samples for illustrating electromechanical coupled process by measuring the transport property when a mechanical strain is applied, such as nanotubes [65–67] and nanowires [68].

Electrochemical properties

Studying electrochemical process is fundamentally important for understanding the charging and discharging processes for energy storage. Direct visualization of the structural transformation as ions being transported can provide quantitative information about the diffusion of ions and a better understanding of the life time of batteries. Recently, Huang *et al.* [69] reported the creation of a nanoscale electrochemical device inside a TEM—consisting of a single tin dioxide (SnO_2) nanowire anode, an ionic liquid electrolyte and a bulk lithium cobalt dioxide ($LiCoO_2$) cathode—and the *in situ* observation of the lithiation of the SnO_2 nanowire during electrochemical charging (Fig. 6). Upon charging, a reaction front propagated progressively along the nanowire, causing the nanowire to swell, elongate

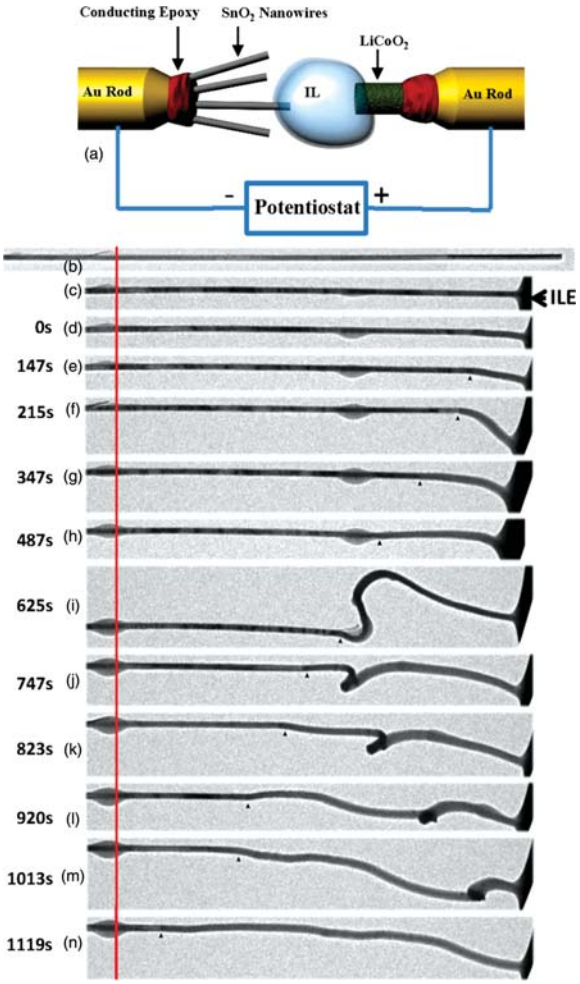

Fig. 6. Time-lapse structure evolution of a SnO_2 nanowire anode during charging at –3.5 V against a $LiCoO_2$ cathode. The single-crystal nanowire was elongated 60% and the diameter increased 45% (resulting in a 240% volume expansion) after charging for 1860 s. (a) Schematic of the experimental setup. The initially straight nanowire (b and c) became significantly twisted and bent after charging (d–n). The chemical reaction front progressed along the nanowire's longitudinal direction, with the front clearly visible, as pointed out by arrowheads (from [69]).

and spiral. The creation of dislocation cloud in the nanowire indicates large in-plane misfit stress which is a structural precursor to electrochemically driven solid-state amorphization. Such an ionic transport has also been studied for ionic conductors such as Ag_2S [70]. Electric-field-driven oxygen diffusion in CeO_2 has been directly correlated to the formation of superlattices as a result of forming ordered vacancies [71].

Magnetic properties

Studying the magnetic properties of nanomaterials in TEM is challenged by the presence of a magnetic

field at the vicinity of the objective lens. By creating a magnetic field-free environment with the use of Lorentz lens with the scarification of magnification and possibly image resolution, the dynamic magnetic properties of a thin film can be studied by creating a local field using tiny coils built around the sample [72]. Such study can reveal the domain width as well as switching speed of the magnetic domain for exploring the limit of magnetic data storage. The current-induced motion of vortices in superconductors and polarons in manganites with colossal magnetoresistance effects has also been studied *in situ* [73].

Electron holography is a powerful tool for imaging magnetic lines in superconducting materials [74]. It is a technique for directly revealing the phase information of the electron wave after interacting with the specimen, and thus can be used to image the ferroelectric domain boundary and magnetic domains.

Photon excitation properties

Photon-induced phase transformation is of great interest in studying photon-matter interaction. Such a process was studied by an *ex situ* technique for revealing the shape transformation and melting of metallic nanoparticles and nanorods [75]. It would be another application of *in situ* TEM if photon excitation can be directly guided to the sample. A number of interesting photon-stimulated processes at metal–semiconductor and semiconductor p–n junctions can be studied by controlling the incident light energy, power and pulses.

Summary

A future TEM is a comprehensive machine that is capable of providing picosecond time-resolved information at picometer-scale spatial resolution. At the same time, physical and chemical properties can be measured from a region as small as a few nanometers by introducing local electric, mechanical, thermal, magnetic and/or photon stimulations/excitations. Studying surface chemical processes at ambient conditions will be an important area for electron microscopy. Furthermore, the introduction of cryostage will allow the above techniques to be applied to biological samples. It is anticipated that nanoscopy and picoscopy will greatly impact materials science, biology, physics and chemistry. It will be a key tool in picoscale science and nanoscale technology.

The major limitations on fulfilling the proposed tasks may include the following factors. The brightness of the electron source and the current density may limit the time resolution to be achieved. The limited space around the specimen area could limit the implementation of several excitation fields for physical property measurements. The introduction of environmental cell could restrict the application of other *in situ* measurement techniques due to restriction of space and the preservation of vacuum. With the development of technology, we are optimistic that better solutions will be found to solve these problems.

Acknowledgements

Thanks are due to Dr Yong Ding for stimulating discussions and help.

Funding

This work was supported by NSF and MANA, NIMS (Japan).

References

1 Hirsch P, Howie A, Nicholson R B, Pashiley D W, and Whelan M J (1965) *Electron microscopy of thin crystals* (Butterworths, London).

2 Buseck P, Cowley J M, and Eyring L (eds.) (1988) *High-resolution transmission electron microscopy and associated techniques* (Oxford University Press, Oxford).

3 Smith D J (2008) Progress and perspectives for atomic-resolution electron microscopy. *Ultramicroscopy* **108**: 159–166.

4 Wang Z L (2003) New developments in transmission electron microscopy for nanotechnology. *Adv. Mater.* **15**: 1497–1514.

5 Newbury D E (1986) *Advanced scanning electron microscopy and X-ray microanalysis* (Plenum Press, New York).

6 Egerton R (1996) *Electron energy-loss spectroscopy in the electron microscope* (Plenum Press, New York).

7 Haider M, Uhlemann S, Schwan E, Rose H, Kabius B, and Urban K (1998) Electron microscopy image enhanced. *Nature* **392**: 768–769.

8 Dellby N, Krivanek O L, Nellist P D, Batson P E, and Lupini A R (2001) Progress in aberration-corrected scanning transmission electron microscopy. *J. Electron. Microsc.* **50**: 177–185.

9 Jia C L and Urban K (2004) Atomic-resolution measurement of oxygen concentration in oxide materials. *Science* **303**: 2001–2004.

10 Shao-Horn Y, Croguennec L, Delmas C, Nelson E C, and O'Keefe M A (2003) Atomic resolution of lithium ions in $LiCoO_2$. *Nat. Mater.* **2**: 464–467.

11 Urban K W (2008) Studying atomic structures by aberration-corrected transmission electron microscopy. *Science* **321**: 506–510.

12 Yu R, Hu L H, Cheng Z Y, Li Y D, Ye H Q, and Zhu J (2010) Direct subangstrom measurement of surfaces of oxide particles. *Phys. Rev. Lett.* **105**: 5–10.

13 Zhu Y, Inada H, Nakamura K, and Wall J (2009) Imaging single atoms using secondary electrons with an aberration-corrected electron microscope. *Nat. Mater.* **8**: 808–812.

14 Wang Z L (1999) Phonon scattering: how does it affect the image contrast in high-resolution transmission electron microscopy? *Phil. Mag. B* **79**: 37–48.

15 Wang Z L (1998) An optical potential approach to incoherent multiple thermal diffuse scattering in quantitative HRTEM. *Ultramicroscopy* **74**: 7–26.

16 Forbes B D, Martin A V, Findlay S D, D'Alfonso A J, and Allen L J (2010) Quantum mechanical model for phonon excitation in electron diffraction and imaging using a Born–Oppenheimer approximation. *Phys. Rev. B* **82**: 104103.

17 Van Dyck D (2009) Is the frozen phonon model adequate to describe inelastic phonon scattering? *Ultramicroscopy* **109**: 677–682.

18 Wang Z L (1998) The 'frozen-lattice' approach for incoherent phonon excitation in electron scattering: how accurate is it? *Acta Crystallogr. A* **54**: 460–467.

19 Cowley J M and Moodie A F (1957) Possibilities for the direct observation of crystal structures. *Acta Crystallogr.* **10**: 752–753.

20 Wang Z L (2003) Thermal diffuse scattering in sub-angstrom quantitative electron microscopy—phenomenon, effects and approaches. *Micron* **34**: 141–155.

21 Rosenauer A, Schowalter M, Titantah J T, and Lamoen D (2008) An emission-potential multislice approximation to simulate thermal diffuse scattering in high-resolution transmission electron microscopy. *Ultramicroscopy* **108**: 1504–1513.

22 Rother A, Gemming T, and Lichte H (2009) The statistics of the thermal motion of the atoms during imaging process in transmission electron microscopy and related techniques. *Ultramicroscopy* **109**: 139–146.

23 Wang Z L (1995) *Elastic and inelastic scattering in electron diffraction and imaging* (Plenum Press, New York).

24 Mkhoyan K A, Maccagnano-Zacher S E, Thomas M G, and Silcox J (2008) Critical role of inelastic interactions in quantitative electron microscopy. *Phys. Rev. Lett.* **100**: 025503.

25 Lebeau J M, Findlay S D, Allen L J, and Stemmer S (2008) Quantitative atomic resolution scanning transmission electron microscopy. *Phys. Rev. Lett.* **100**: 206101.

26 Wang Z L (1993) Thermal diffuse-scattering in high-resolution electron holography. *Ultramicroscopy* **52**: 504–511.

27 Lehman M, Geiger D, Buscher I, Zandbergen H W, Van Dyck D, and Lichte H (2002) 15th Internationl Congress on Electron Microscopy, ICEM15, Durban. South Africa, 3.

28 Crewe A V, Isaacson M, and Johnson D (1970) Secondary electron detection in a field emission scanning microscope. *Rev. Sci. Instrum.* **41**: 20–27.

29 Cowley J M (1976) Scanning-transmission electron-microscopy of thin specimens. *Ultramicroscopy* **2**: 3–16.

30 Muller D A, Kourkoutis L F, Murfitt M, Song J H, Hwang H Y, Silcox J, Dellby N, and Krivanek O L (2008) Atomic-scale chemical imaging of composition and bonding by aberration-corrected microscopy. *Science* **319**: 1073–1076.

31 Pennycook S J and Boatner L A (1988) Chemically sensitive structure-imaging with a scanning-transmission electron-microscope. *Nature* **336**: 565–567.

32 Wang Z L and Cowley J M (1989) Simulating high-angle annular dark-field stem images including inelastic thermal diffuse-scattering. *Ultramicroscopy* **31**: 437–454.

33 Klenov D O and Stemmer S (2006) Contributions to the contrast in experimental high-angle annular dark-field images. *Ultramicroscopy* **106**: 889–901.

34 Wang Z L (1995) Dynamical theories of dark-field imaging using diffusely scattered electrons in STEM and TEM. *Acta Crystallogr. A* **51**: 569–585.

35 Zewail A H (2006) 4D ultrafast electron diffraction, crystallography, and microscopy. *Annu. Rev. Phys. Chem.* **57**: 65–103.

36 Campbell G H, Lagrange T, Kim J S, Reed B W, and Browning N D (2010) Quantifying transient states in materials with the dynamic transmission electron microscope. *J. Electron. Microsc.* **59**: S67–S74.

37 Yang D-S, Lao C S, and Zewail A H (2008) 4D electron diffraction reveals correlated unidirectional behavior in zinc oxide nanowires. *Science* **321**: 1660–1664.

38 Barwick B, Park H S, Kwon O H, Baskin J S, and Zewail A H (2008) 4D imaging of transient structures and morphologies in ultrafast electron microscopy. *Science* **322**: 1227–1231.

39 Zhao J O, Huang J Q, Wei F, and Zhu J (2010) Mass transportation mechanism in electric-biased carbon nanotubes. *Nano Lett.* **10**: 4309–4315.

40 Howe J M, Mori H, and Wang Z L (2008) *In situ* high-resolution transmission electron microscopy in the study of nanomaterials and properties. *MRS Bull.* **33**: 115–121.

41 Poncharal P, Wang Z L, Ugarte D, and De Heer W A (1999) Electrostatic deflections and electromechanical resonances of carbon nanotubes. *Science* **283**: 1513–1516.

42 Wang Z L, Poncharal P, and De Heer W A (2000) Nanomeasurements of individual carbon nanotubes by *in situ* TEM. *Pure Appl. Chem.* **72**: 209–219.

43 Ferreira P J, Mitsuishi K, and Stach E A (2008) *In situ* transmission electron microscopy. *MRS Bull.* **33**: 83–85.

44 Haque M A, Espinosa H D, and Lee H J (2010) MEMS for *in situ* testing-handling, actuation, loading, and displacement measurements. *MRS Bull.* **35**: 375–381.

45 Gao R P, Wang Z L, Bai Z G, De Heer W A, Dai L M, and Gao M (2000) Nanomechanics of individual carbon nanotubes from pyrolytically grown arrays. *Phys. Rev. Lett.* **85**: 622–625.

46 Stach E A, Freeman T, Minor A M, Owen D K, Cumings J, Wall M A, Chraska T, Hull R, Morris J W, Zettl A, and Dahmen U (2001) Development of a nanoindenter for *in situ* transmission electron microscopy. *Microsc. Microanal.* **7**: 507–517.

47 Oh S H, Legros M, Kiener D, and Dehm G (2009) *In situ* observation of dislocation nucleation and escape in a submicrometre aluminium single crystal. *Nat. Mater.* **8**: 95–100.

48 Shan Z W, Mishra R K, Asif S A S, Warren O L, and Minor A M (2008) Mechanical annealing and source-limited deformation in submicrometre-diameter Ni crystals. *Nat. Mater.* **7**: 115–119.

49 Robertson I M, Ferreira P J, Dehm G, Hull R, and Stach E A (2008) Visualizing the behavior of dislocations—seeing is believing. *MRS Bull.* **33**: 122–131.

50 Legros M, Gianola D S, and Motz C (2010) Quantitative *in situ* mechanical testing in electron microscopes. *MRS Bull.* **35**: 354–360.

51 Zheng H, Cao A J, Weinberger C R, Huang J Y, Du K, Wang J B, Ma Y Y, Xia Y N, and Mao X S (2010) Discrete plasticity in sub-10-nm-sized gold crystals. *Nat. Commun.* **1:** doi:10.1038/ncomms1149.

52 Han X D, Zhang Y F, Zheng K, Zhang X N, Zhang Z, Hao Y J, Guo X Y, Yuan J, and Wang Z L (2007) Low-temperature *in situ* large strain plasticity of ceramic sic nanowires and its atomic-scale mechanism. *Nano Lett.* **7**: 452–457.

53 Han X D, Zheng K, Zhang Y F, Zhang X N, Zhang Z, and Wang Z L (2007) Low-temperature *in situ* large-strain plasticity of silicon nanowires. *Adv. Mater.* **19**: 2112–2118.

54 Zheng K, Wang C C, Cheng Y Q, Yue Y H, Han X D, Zhang Z, Shan Z W, Mao S X, Ye M M, Yin Y D, and Ma E (2010)

Electron-beam-assisted superplastic shaping of nanoscale amorphous silica. *Nat. Commun.* **1**: doi:10.1038/ncomms1021.

55 Wang Z L, Poncharal P, and De Heer W A (2000) Measuring physical and mechanical properties of individual carbon nanotubes by *in situ* TEM. *J. Phys. Chem. Solids* **61**: 1025–1030.

56 Gaiboyes P L (1992) Defects in oxide catalysts—fundamental-studies of catalysis in action. *Catal. Rev.* **34**: 1–54.

57 Hansen P L, Wagner J B, Helveg S, Rostrup-Nielsen J R, Clausen B S, and Topsoe H (2002) Atom-resolved imaging of dynamic shape changes in supported copper nanocrystals. *Science* **295**: 2053–2055.

58 Sharma R (2001) Design and applications of environmental cell transmission electron microscope for *in situ* observations of gas–solid reactions. *Microsc. Microanal.* **7**: 494–506.

59 Gai P L, Sharma R, and Ross F M (2008) Environmental (S)TEM studies of gas–liquid–solid interactions under reaction conditions. *MRS Bull.* **33**: 107–114.

60 Takahashi Y, Tanaka M, Higashida K, Yasuda K, Matsumura S, and Noguchi H (2010) A combined environmental straining specimen holder for high-voltage electron microscopy. *Ultramicroscopy* **110**: 1420–1427.

61 Simonsen S B, Chorkendorff I, Dahl S, Skoglundh M, Sehested J, and Helveg S (2010) Direct observations of oxygen-induced platinum nanoparticle ripening studied by *in situ* TEM. *J. Am. Chem. Soc.* **132**: 7968–7975.

62 Wen C Y, Reuter M C, Bruley J, Tersoff J, Kodambaka S, Stach E A, and Ross F M (2009) Formation of compositionally abrupt axial heterojunctions in silicon–germanium nanowires. *Science* **326**: 1247–1250.

63 Kondo Y and Takayanagi K (2000) Synthesis and characterization of helical multi-shell gold nanowires. *Science* **289**: 606–608.

64 Ohnishi H, Kondo Y, and Takayanagi K (1998) Quantized conductance through individual rows of suspended gold atoms. *Nature* **395**: 780–783.

65 Xu Z, Golberg D, and Bando Y (2009) *In Situ* TEM–STM recorded kinetics of boron nitride nanotube failure under current flow. *Nano Lett.* **9**: 2251–2254.

66 Golberg D, Costa P M F J, Lourie O, Mitome M, Bai X D, Kurashima K, Zhi C Y, Tang C C, and Bando Y (2007) Direct force measurements and kinking under elastic deformation of individual multiwalled boron nitride nanotubes. *Nano Lett.* **7**: 2146–2151.

67 Jaroenapibal P, Jung Y, Evoy S, and Luzzi D E (2009) Electromechanical properties of individual single-walled carbon nanotubes grown on focused-ion-beam patterned substrates. *Ultramicroscopy* **109**: 167–171.

68 Andzane J, Petkov N, Livshits A I, Boland J J, Holmes J D, and Erts D (2009) Two-terminal nanoelectromechanical devices based on germanium nanowires. *Nano Lett.* **9**: 1824–1829.

69 Huang J Y, Zhong L, Wang C M, Sullivan J P, Xu W, Zhang L Q, Mao S X, Hudak N S, Liu X H, Subramanian A, Fan H Y, Qi L A, Kushima A, and Li J (2010) *In situ* observation of the electrochemical lithiation of a single SnO_2 nanowire electrode. *Science* **330**: 1515–1520.

70 Xu Z, Bando Y, Wang W L, Bai X D, and Golberg D (2010) Real-time *in situ* HRTEM-resolved resistance switching of Ag_2S nanoscale ionic conductor. *ACS Nano* **4**: 2515–2522.

71 Gao P, Wang Z Z, Fu W Y, Liao Z L, Liu K H, Wang W L, Bai X D, and Wang E (2010) *In situ* TEM studies of oxygen vacancy migration for electrically induced resistance change effect in cerium oxides. *Micron* **41**: 301–305.

72 Cumings J, Olsson E, Petford-Long A K, and Zhu Y M (2008) Electric and magnetic phenomena studied by *in situ* transmission electron microscopy. *MRS Bull.* **33**: 101–106.

73 Jooss C, Wu L, Beetz T, Klie R F, Beleggia M, Schofield M A, Schramm S, Hoffmann J, and Zhu Y (2007) Polaron melting and ordering as key mechanisms for colossal resistance effects in manganites. *Proc. Natl Acad. Sci. USA* **104**: 13597–13602.

74 Tonomura A (1999) *Electron holography* (Springer, Berlin).

75 Link S, Wang Z L, and El-Sayed M A (2000) How does a gold nanorod melt? *J. Phys. Chem. B* **104**: 7867–7870.